Stem Cell Reports
Article
OPEN ACCESS

Modeling Hippocampal Neurogenesis Using Human Pluripotent Stem Cells

Diana Xuan Yu,[1] Francesco Paolo Di Giorgio,[2] Jun Yao,[1] Maria Carolina Marchetto,[1] Kristen Brennand,[3] Rebecca Wright,[1] Arianna Mei,[1] Lauren Mchenry,[1] David Lisuk,[1] Jaeson Michael Grasmick,[1] Pedro Silberman,[1] Giovanna Silberman,[1] Roberto Jappelli,[1] and Fred H. Gage[1,*]

[1]The Salk Institute for Biological Studies, 10010 North Torrey Pines Road, La Jolla, CA 92037, USA
[2]Neuroscience Discovery, Novartis Pharma AG, Novartis Institute for Biomedical Research, Postfach, Basel CH-4002, Switzerland
[3]Department of Neuroscience/Psychiatry, Mount Sinai School of Medicine, 1425 Madison Ave, New York, NY 10059, USA
*Correspondence: gage@salk.edu
http://dx.doi.org/10.1016/j.stemcr.2014.01.009

SUMMARY

The availability of human pluripotent stem cells (hPSCs) offers the opportunity to generate lineage-specific cells to investigate mechanisms of human diseases specific to brain regions. Here, we report a differentiation paradigm for hPSCs that enriches for hippocampal dentate gyrus (DG) granule neurons. This differentiation paradigm recapitulates the expression patterns of key developmental genes during hippocampal neurogenesis, exhibits characteristics of neuronal network maturation, and produces PROX1+ neurons that functionally integrate into the DG. Because hippocampal neurogenesis has been implicated in schizophrenia (SCZD), we applied our protocol to SCZD patient-derived human induced pluripotent stem cells (hiPSCs). We found deficits in the generation of DG granule neurons from SCZD hiPSC-derived hippocampal NPCs with lowered levels of *NEUROD1*, *PROX1*, and *TBR1*, reduced neuronal activity, and reduced levels of spontaneous neurotransmitter release. Our approach offers important insights into the neurodevelopmental aspects of SCZD and may be a promising tool for drug screening and personalized medicine.

INTRODUCTION

The advent of stem cell biology has opened new avenues in the field of neuroscience research as well as therapeutic approaches for neurological diseases. Although it is clear that human pluripotent stem cells (hPSCs; i.e., both human embryonic stem cells [hESCs] and human induced pluripotent stem cells [hiPSCs]) can give rise to functional neurons, a current challenge is to develop differentiation strategies that can produce disease-relevant subtypes of neurons. To date, progress has been made to generate enriched populations of ventral midbrain dopaminergic neurons and spinal motor neurons to model Parkinson disease and amyotrophic lateral sclerosis, respectively (Perrier et al., 2004; Roy et al., 2006; Di Giorgio et al., 2008; Dimos et al., 2008; Marchetto et al., 2008; Kriks et al., 2011; Ma et al., 2011). In addition, cortical pyramidal neurons and forebrain interneurons have been generated from hiPSCs (Shi et al., 2012a,b; Vanderhaeghen, 2012; Maroof et al., 2013; Nicholas et al., 2013). Most of these methods induce differentiation that approximates the in vivo developmental program. Consequently, in addition to producing a neuronal subtype, hPSCs can potentially recapitulate the developmental stages of the neuron of interest (Hu et al., 2010; Shi et al., 2012b; Nicholas et al., 2013) and provide insights into the pathogenesis of neurodevelopmental diseases where deficits originate in developmental windows prior to the onset of clinical symptoms.

The dentate gyrus (DG) of the hippocampus is one of two areas of the brain where neurogenesis continues to occur throughout life. New neurons generated at the subgranular zone (SGZ) of the DG integrate play a fundamental role in learning and memory (Zhao et al., 2008). Aberrations in hippocampal neurogenesis have been implicated in epileptic seizures (Jessberger et al., 2007), Alzheimer disease (Tatebayashi et al., 2003), and cognitive defects characteristic of depression (Sahay and Hen, 2007; Mateus-Pinheiro et al., 2013) and schizophrenia (SCZD) (Reif et al., 2006; Tamminga et al., 2010; Walton et al., 2012; Hagihara et al., 2013). Unfortunately, it is difficult to investigate the early events of these central nervous system (CNS) disorders in the human system, and it is not clear whether findings from studies using rodent models will translate across species.

Here, we present a differentiation paradigm that produces an enriched population of hippocampal DG granule neurons using key developmental cues that specify the hippocampal DG identity. Using two differentiation approaches based on free-floating embryoid bodies (EBs) and neural progenitor cell (NPC) monolayers, we generated neurons expressing PROX1 and TBR1, markers found in mature DG granule neurons (Hodge et al., 2012; Iwano et al., 2012). The differentiation process recapitulates expression patterns of key developmental genes, including *NEUROD1* and *DCX*, that are critical for hippocampal neurogenesis (Miyata et al., 1999; Liu et al., 2000; Schwab et al., 2000; Gao et al., 2009). Furthermore, these neurons

formed functional networks characteristic of granule neuron maturation and are able to functionally integrate into the endogenous DG upon in vivo transplantation. To test the effectiveness of this protocol to uncover functional defects in human diseased neurons, we used this differentiation paradigm on SCZD patient hiPSCs and control hiPSCs as a proof-of-principle application. We found deficits in the generation of hippocampal granule neurons from SCZD hiPSC-derived hippocampal NPCs with reduced levels of *PROX1* and *TBR1*. Furthermore, SCZD granule neurons showed deficits in neuronal activity, as evidenced by the reduced frequency of spontaneous neurotransmitter release. Our strategy to generate a specific, disease-relevant subtype of neurons reduces the variability within the cellular population being examined and allows for the detection of early alterations in the developing SCZD hippocampal granule neurons. This approach may offer important insights into the neurodevelopmental aspects of SCZD and presents a promising tool for drug screening, diagnosis, and personalized medicine.

RESULTS

To develop a differentiation paradigm that enriches for hippocampal granule neurons, we first utilized free-floating EBs, which provide 3D spatial cues that have been shown to simulate aspects of pregastrulation development and early gastrulation (Kopper et al., 2010). The differentiation approach was optimized based on key morphological cues that specify the hippocampal DG identity during development. Mimicking the developmental signals that generate the anterior-posterior patterning of the forebrain, we first treated the EBs with a cocktail of anticaudalizing factors (DKK1, noggin, and SB431542) blocking the WNT, bone morphogenetic protein (BMP), and transforming growth factor-β (TGF-β) pathways to obtain telencephalic neural precursors (Watanabe et al., 2005). In addition, we applied cyclopamine, an antagonist of the Sonic Hedgehog pathway, to enrich for dorsal forebrain progenitors (Gaspard et al., 2008) (Figure 1A). After 20 days, the mature EBs were treated with Wnt3a, a WNT protein previously shown to be important for the maintenance of hippocampal progenitors and their differentiation into DG granule neurons (Lee et al., 2000; Machon et al., 2007; Kuwabara et al., 2009; Wexler et al., 2009; Karalay et al., 2011), as well as brain-derived growth factor (BDNF), a neurotrophic factor found to promote hippocampal neurogenesis throughout life (Scharfman et al., 2005; Erickson et al., 2010) (Figure 1A).

After 35 days of differentiation, we observed expression of TUJ1 and MAP2AB in the EBs, indicating the derivation of neurons using the differentiation paradigm (Figure 1B). Strikingly, we detected a significant expression of PROX1 in the EBs (~32%), a marker specific to DG granule neurons in the hippocampus (Hodge et al., 2012; Iwano et al., 2012), compared to the untreated group (~4.7%) (Figures 1B and 1C). We further confirmed this observation using quantitative RT-PCR (qRT-PCR), which showed a remarkable increase in *PROX1* expression (Figure 1E) and a significant reduction in *OCT4* expression in EBs treated with the cocktail of factors (Figure 1D).

To further authenticate the generation of DG granule neurons using this protocol, we assessed the EBs at various time points to track the development of these neurons during the differentiation process. Previous studies of both embryonic and adult neurogenesis in the DG have revealed a number of transcription factors, as well as their expression patterns, that are important for directing neuronal fate specification and lineage commitment during hippocampal neurogenesis (Hodge et al., 2012; Hsieh, 2012). We examined the expression dynamics of these key markers to determine the extent to which our protocol for in vitro differentiation recapitulated the in vivo neurogenesis process. Following 10 days of differentiation, we observed upregulated expression levels of *EMX2*, *FOXG1*, and *PAX6*, which are markers found in hippocampal NPCs (Pellegrini et al., 1996; Shinozaki et al., 2004; Shen et al., 2006; Osumi et al., 2008), together with *NEUROD1*, an indispensable transcriptional activator that regulates neuronal differentiation of granule neurons in the hippocampus (Miyata et al., 1999; Liu et al., 2000; Schwab et al., 2000; Gao et al., 2009) (Figure 1F). These hippocampal NPCs further matured into neuroblasts and postmitotic granule neurons, as indicated by the increasing levels of *DCX* and *TBR1*, together with *PROX1*, after 20 days of differentiation (Figures 1E and 1G). Taken together, these data indicate that we were able to obtain PROX1+ hippocampal granule neurons from hESCs and that these neurons were generated via a process that recapitulated important aspects of hippocampal neurogenesis in vivo. We then dissociated the EBs after 40 days of differentiation and coculture with human hippocampal astrocytes to allow formation of neural networks and facilitate further neuronal maturation. As a result, we observed neurons that had extensively branched dendritic arbors and were triple positive for PROX1, MAP2AB, and NEUN, indicative of postmitotic hippocampal granule neurons (Figures 1H and 1I).

hESC-Derived Hippocampal NPCs Can Give Rise to DG Granule Neurons

We further adapted our protocol to utilize NPC monolayers during differentiation. To this end, we plated EBs treated with anticaudalizing factors onto laminin/polyornithine-coated tissue culture surfaces at differentiation day 20 to

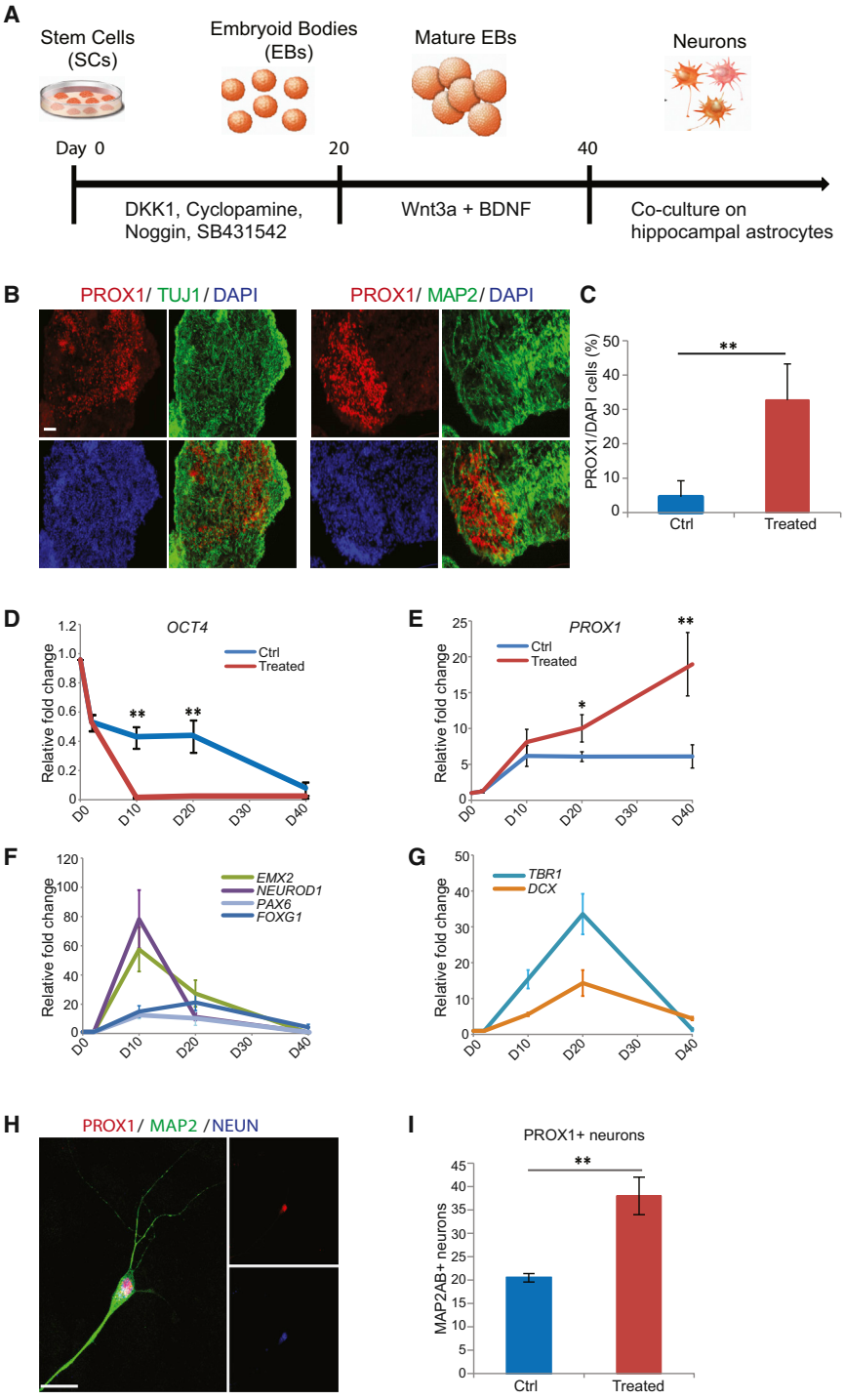

Figure 1. Generation of Hippocampal Granule Neurons from hESCs Using Embryoid Bodies

(A) Schematic representation of the differentiation paradigm for generating hippocampal granule neurons using free-floating embryoid bodies (EBs).

(B) Immunostaining of EB cross sections at differentiation day 35 showed the presence of PROX1 with TUJ1 and MAP2AB. Scale bar, 100 μm.

(C) Quantification of PROX1+ immunostaining in EBs at differentiation day 35 showed a higher percentage of PROX1+ nuclei in EBs treated with cocktail of factors. n = 3 biological replicates; two-tailed t-test.

(D) qPCR for OCT4 expression in control and treated EBs over time.

(E) qPCR for *PROX1* expression in control and treated EBs over time.

(F) Expression patterns of genes *EMX2*, *PAX6*, *FOXG1*, and *NEUROD1* found in hippocampal neural progenitors.

(G) Expression patterns of genes *DCX* and *TBR1* found in the immature and mature hippocampal granule neurons.

(H) Immunostaining of hippocampal granule neurons dissociated from EBs at differentiation day 40 and cocultured with hippocampal astrocytes for 4 weeks. Scale bar, 15 μm.

(I) Quantification of immunostaining in 4-week cocultures showed an increased number of PROX1+ neurons in treated cultures.

*p < 0.05; **p < 0.01. In (C) and (I), n = 3 biological replicates; two-tailed t test. In (D)–(G), n = 3 biological replicates; two-way ANOVA and Bonferroni post hoc test. All data are presented as mean ± SEM.

allow rosette formation. The rosettes were manually dissociated after 1 week to isolate the NPC population (Figure 2A). Using immunostaining and quantitative PCR (qPCR), we found that the NPCs obtained using this method showed similar levels of SOX2 but higher levels of the hippocampal NPC markers PAX6, FOXG1, and EMX2 compared to NPCs derived without the anticaudalizing cocktail treatment (Figures 2B and 2C).

We then differentiated the hippocampal NPCs into DG granule neurons by using Wnt3a and BDNF, two soluble factors that have been shown to be essential for the generation and maturation of DG granule neurons. Our results

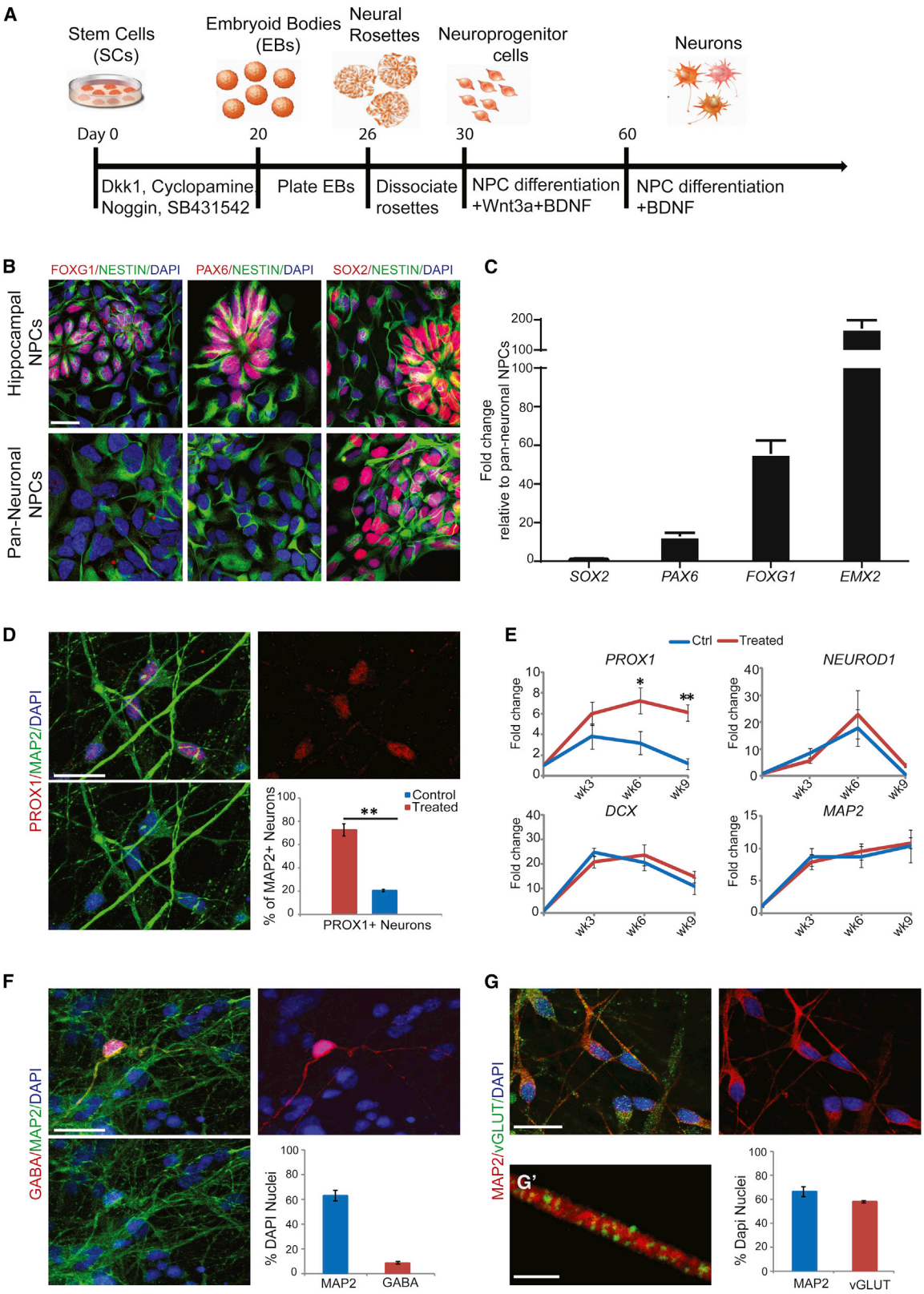

(legend on next page)

showed that whereas the NPCs were able to give rise to neurons as indicated by transiently increased levels of *NEUROD1* and *DCX* as well as a steadily increased level of *MAP2AB*, *PROX1* levels were significantly higher in cultures treated with Wnt3a and BDNF (Figure 2E). Furthermore, immunostaining analysis with vGLUT, a glutamatergic neuronal marker, and GABA, a GABAergic neuronal marker, showed that our protocol produced predominantly glutamatergic neurons (>85%) (Figures 2G and 2G′), with low occurrence of GABAergic neurons (<15%) (Figure 2F). Quantitative analysis for colabeling of PROX1 and MAP2AB revealed a significantly higher number of PROX1+ neurons in Wnt3a/BDNF-treated cultures (~70%) compared to the control cultures (~20%) (Figure 2D).

In Vitro Hippocampal Neurogenesis Can Capture Developmental Stages of Neural Network Maturation

We next determined the functional characteristics of the neurons using electrophysiology and calcium imaging. After 4 weeks of differentiation on hippocampal astrocytes, whole-cell patch-clamp recording revealed that the PROX1+ cells showed characteristics of functional neurons, such as normal levels of transient sodium inward currents and sustained potassium outward currents induced by voltage step depolarization (Figure 3A); the cells were able to fire action potentials following somatic current injection (Figure 3C). Importantly, a majority of the neurons (eight out of ten) were functionally active, with spontaneous bursts of action potentials (Figure 3B) as well as spontaneous postsynaptic currents (Figure 3D–3F), indicating formation of functional neural networks. Because spontaneous neuronal activity leads to increases in intracellular calcium levels and activation of signaling pathways that are important for the regulation of neuronal processes (Spitzer et al., 2004), we next turned to calcium imaging to evaluate the maturation of the hESC-derived hippocampal neural networks at 3 weeks and 6 weeks postdifferentiation. We observed a significantly increased percentage of active neurons as well as a higher frequency of calcium transients at 6 weeks versus 3 weeks postdifferentiation, indicating maturation of the neuronal population and increased levels of network activity (Figure 4B). These intracellular calcium transients could be blocked by the Na^+ channel blocker tetrodotoxin (TTX), verifying its correlation with neuronal activity (Figures 4C, 4D, and 4H).

Because the mature hippocampal granule neurons in our system were almost exclusively glutamatergic, we employed pharmacological perturbation during calcium imaging to further assess the dependency of the network activity on glutamate-mediated synaptic transmission. Application of APV, an antagonist of NMDA receptor (NMDAR), and CNQX, an antagonist of AMPA receptor, reduced the neuronal network activity, as indicated by a decrease in the proportion of signaling neurons as well as their calcium transient frequency. Importantly, we observed a greater sensitivity of the networks to APV at the 3-week time point, whereas CNQX exerted a greater effect at the 6-week time point (Figures 4C–4F). This observation is consistent with previous work on synaptic maturation of hippocampal granule neurons that indicated a transition from an NDMA-receptor to an AMPA-receptor-mediated excitatory transmission as the granule neurons mature and integrate into the existing circuitry (Tashiro et al., 2006). Finally, studies have also shown a transition in hippocampal granule neurons from a GABA-excitatory to a GABA-inhibitory state during early maturation as a result of changes in intracellular Cl^- concentration due to the upregulation of the KCC2 channel (Ganguly et al., 2001; Li et al., 2012). In our hands, GABA inhibited the network activity of neurons at both 3 and 6 weeks, with greater reduction at the 6-week postdifferentiation, further indicating the maturation of the neuronal population (Figures 4C, 4D, and 4G).

Hippocampal NPCs Can Generate Prox1+ Neurons that Morphologically Integrate into the DG In Vivo

Our results indicated that hippocampal NPCs were able to generate neurons with phenotypic markers and functional

Figure 2. Generation of Hippocampal Granule Neurons from hESCs Using Monolayer Neural Progenitor Cells

(A) Schematic representation of the differentiation paradigm for generating hippocampal granule neurons using neural progenitor cells (NPCs).

(B) Representative images showing the presence of FOXG1, PAX6, and SOX2 in hESC-derived hippocampal NPCs compared to pan-neuronal NPCs generated without a cocktail of factors. Scale bar, 20 μm.

(C) qPCR showing increased levels of *PAX6*, *FOXG1*, and *EMX2* in hESC-derived hippocampal NPCs.

(D) Representative image and quantification of PROX1+ neurons at differentiation week 5. Scale bar, 30 μm.

(E) qPCR for expression pattern of genes relevant to hippocampal neurogenesis.

(F) Representative image and quantification of GABAergic neurons at differentiation week 5. Scale bar, 30 μm.

(G) Representative image and quantification of glutamatergic neurons at differentiation week 5Scale bar, 30 μm. (G′) High-magnification image of vGLUT puncta on a Map2+ dendrite. Scale bar, 3 μm.

*$p < 0.05$, **$p < 0.01$. In (D), n = 3 biological replicates, two-tailed t test. In (C), (F), and (G), n = 3 biological replicates. In (E), n = 3 biological replicates; two-way ANOVA and Bonferroni post hoc test. All data are presented as mean ± SEM.

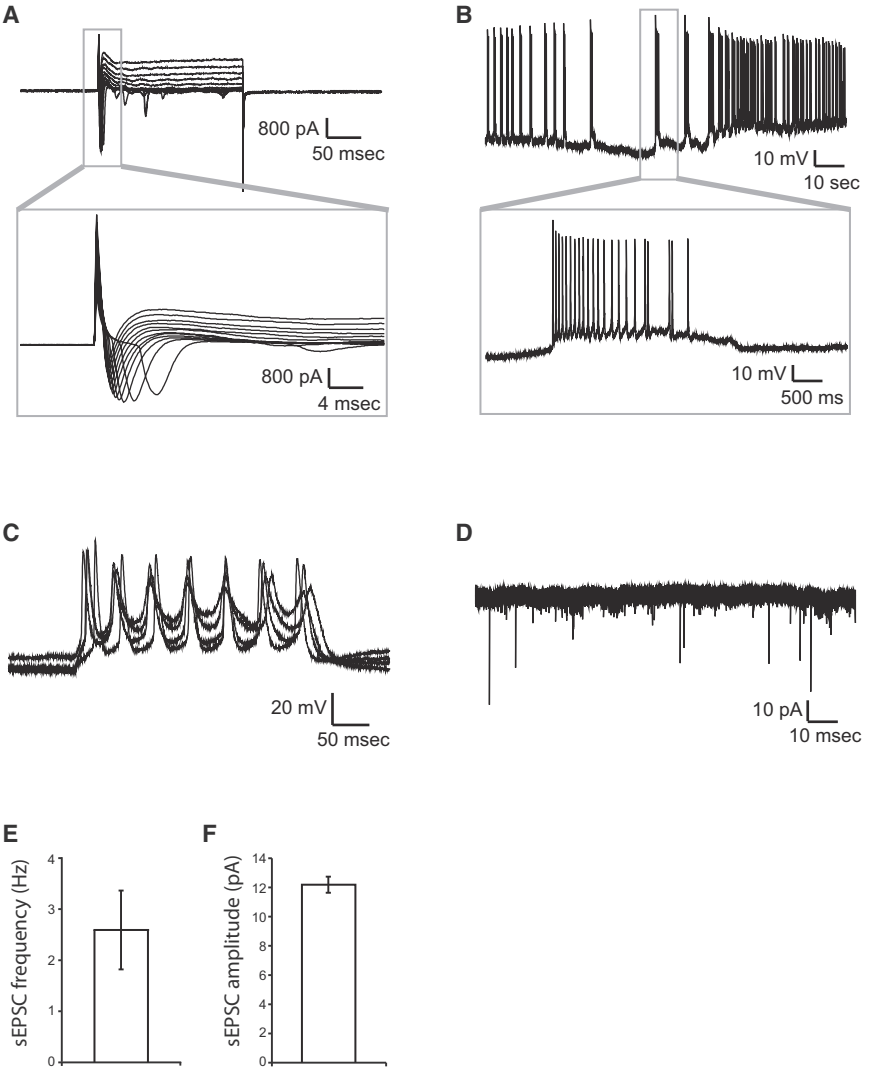

Figure 3. Whole-Cell Patch-Clamp Recordings of hESC-Derived Hippocampal Granule Neurons at Differentiation Week 4

(A–D) The majority of the neurons patched (eight out of ten) showed Na^+/K+ currents (A) and evoked action potentials (C) as well as spontaneous bursts of action potentials (B) and spontaneous postsynaptic currents (D).

(E and F) Quantification of the frequency and amplitude of spontaneous postsynaptic currents in hESC-derived hippocampal granule neurons at 4 weeks postdifferentiation.

All data are presented as mean ± SEM.

properties that were characteristic of mature DG granule neurons. Next, we determined whether these neurons were able to integrate into the DG in vivo. The hippocampal DG is unique in that it continues to mature during the first 2 weeks of postnatal development in rodents (Hollrigel and Soltesz, 1997). Therefore, we grafted hippocampal NPCs labeled with chicken β-actin (CAG) enhanced green fluorescent protein (EGFP) lentiviral vector into the hippocampus of postnatal day 12 NOD-SCID mice. At 6 weeks posttransplantation, we observed extensive integration of GFP+ cells into the granular cell layer (GCL) of the DG (Figure 5A). We verified the origin of these GFP+ cells using human nuclei (HuNu) staining in the DG of the host tissue (Figure 5C). Quantification of GFP+ cells in the GCL showed that majority of these grafted cells (>80%) stained positive for the neuronal marker, TUJ1, and ~40% were also positive for the DG granule neuron marker, PROX1 (Figure 5B). These grafted neurons had cell bodies within the GCL and branching processes in the molecular layer, which is the region of their inputs from the perforant path. They also sent extensive processes, as labeled by human neurofilament (Steinbeck et al., 2012), to the CA3 regions along the mossy fiber path (Figure 5D). These grafted neurons demonstrated remarkable changes in morphological complexity between 2 and 6 weeks posttransplantation (Figures 5I and 5J). Quantitative analysis of the development of these neurons in vivo using Neurolucida morphometrics revealed significant increases in the soma size, total dendrite length, and branching at 6 weeks compared to 2 weeks posttransplantation, indicating that the transplanted hippocampal NPCs were able to engraft and develop in the DG in vivo (Figures 5K and 5L). Whole-cell patch-clamp recordings of transplanted neurons at 6 months postsurgery showed transient sodium inward current and sustained potassium outward currents induced by voltage step depolarization (Figure 5E) as well

as action potential firing following somatic current injections (Figure 5F). Furthermore, these neurons demonstrated spontaneous postsynaptic currents (Figure 5G) and induced excitatory postsynaptic currents (EPSCs) following stimulation of the perforant path (Figure 5H), indicating functional integration of the grafted cells into the local neural circuitry.

Reduced Levels of Hippocampal Neurogenesis from SCZD NPCs

Alterations in hippocampal neurogenesis have been implicated in SCZD (Tamminga et al., 2010). We have previously demonstrated a decrease in connectivity in SCZD neurons using a rabies virus (Brennand et al., 2011) but did not find a corresponding electrophysiological deficit. In addition, in our previous work, we used a single mature time point to examine these differences, not taking advantage of the temporal differentiation that can be measured in vitro. Thus, we used our hippocampal DG differentiation paradigm to model SCZD-associated defects in hippocampal neurogenesis as a proof-of-principle application. We applied the EB-based hippocampal differentiation approach to hiPSC lines previously derived from four SCZD patients and four control individuals (Brennand et al., 2011). From the panel of hippocampal neurogenesis markers that were assessed, we observed a trend for reduced expression levels of Emx2 and Pax6 (Figures 6A and 6B) in SCZD hiPSCs compared to control hiPSCs. However, the expression levels of *NEUROD1* and *PROX1* in the SCZD lines were significantly lower compared to the controls (Figures 6D and 6E). Furthermore, the expression of *TBR1*, a transcription factor found in postmitotic DG neurons (Hodge et al., 2012), was also significantly reduced in the SCZD neurons (Figure 6F), indicating that there might be defects in the generation of DG granule neurons from the NPC population. Interestingly, the expression of *FOXG1* was also lower in the SCZD lines than in the controls (Figure 6C). Because *FOXG1* has been previously shown to play important roles in both NPC proliferation and survival of newborn DG granule neurons (Shen et al., 2006), this finding was suggestive of potential contributing factors leading to the deficits in hippocampal neurogenesis by the SCZD lines.

Because these findings strongly indicated that, even though SCZD hiPSC lines were capable of generating hippocampal NPCs, there might be defects in the development of these NPCs into DG granule neurons, we assessed the function of SCZD and control hiPSC-derived neurons using calcium imaging. After differentiating SCZD and control hiPSC-derived NPCs for 4 weeks on hippocampal astrocytes, we obtained PROX1+ granule neurons in both groups (Figures 6G and 6H). Calcium imaging of these neural networks at 4 weeks postdifferentiation revealed a significant reduction in the proportion of active neurons in the SCZD group (~57%) compared to the controls (~82%) (Figures 6I and 6J), indicating that the deficits in hippocampal neurogenesis by SCZD lines also affected the neural networks formed by SCZD hiPSCs, potentially resulting in the reduction in connectivity observed in our previous work (Brennand et al., 2011).

SCZD Neurons Show Attenuated Spontaneous Neurotransmitter Release

To further verify our findings on the deficit in development of hippocampal granule neurons carrying the SCZD genetic background, we investigated the synaptic function of the hiPSC-derived PROX1+ neurons that were differentiated for at least 4 weeks in culture on hippocampal astrocytes using whole-cell patch-clamp recordings. To specifically assess the hippocampal granule neurons, cells indicated by a lentiviral *PROX1-EGFP* reporter construct were selected for recording (Figures 7A and 7B; Figure S1 available online). Similar to the control hiPSC-derived neurons, the SCZD PROX1+ neurons showed normal levels of transient sodium inward currents and sustained potassium outward currents evoked by voltage step depolarization (Figures 1C and 7D), and they were able to fire action potentials in response to somatic current injection (Figures 7E and 7F). These observations indicated that the PROX1+ granule cells derived from the SCZD hiPSCs lines showed functional features of neurons. Interestingly, quantitative measurements of spontaneous neurotransmitter release revealed a significant decrease in the frequency of the spontaneous ESPCs (sEPSCs) in the SCZD neural network (Figure 7H; 0.76 ± 0.14 Hz, $n = 42$, $p < 0.003$) compared to the control neurons (3.0 ± 0.70 Hz, $n = 40$) as well as a significant reduction in the amplitude of the sEPSCs (Figure 7H; SCZD, 13.66 ± 1.05 pA; control, 17.66 ± 1.60 pA; $p < 0.05$). Thus, consistent with a previous study (Brennand et al., 2011), our data suggested that delayed conversion of SCZD NPCs into hippocampal granule neurons resulted in the attenuated functional network connectivity and activity levels observed in the SCZD hiPSC-derived neuronal culture.

DISCUSSION

Modeling CNS disorders using hiPSCs holds great potential for elucidating pathogenic mechanisms and identifying potential targets for drug discovery. However, a major challenge to accurately capturing disease-relevant phenotypes using patient-derived hiPSCs is the variability that arises from the heterogeneity in the cellular subtype and the maturation stage of the differentiated neuronal population. In this study, we report directed differentiation of

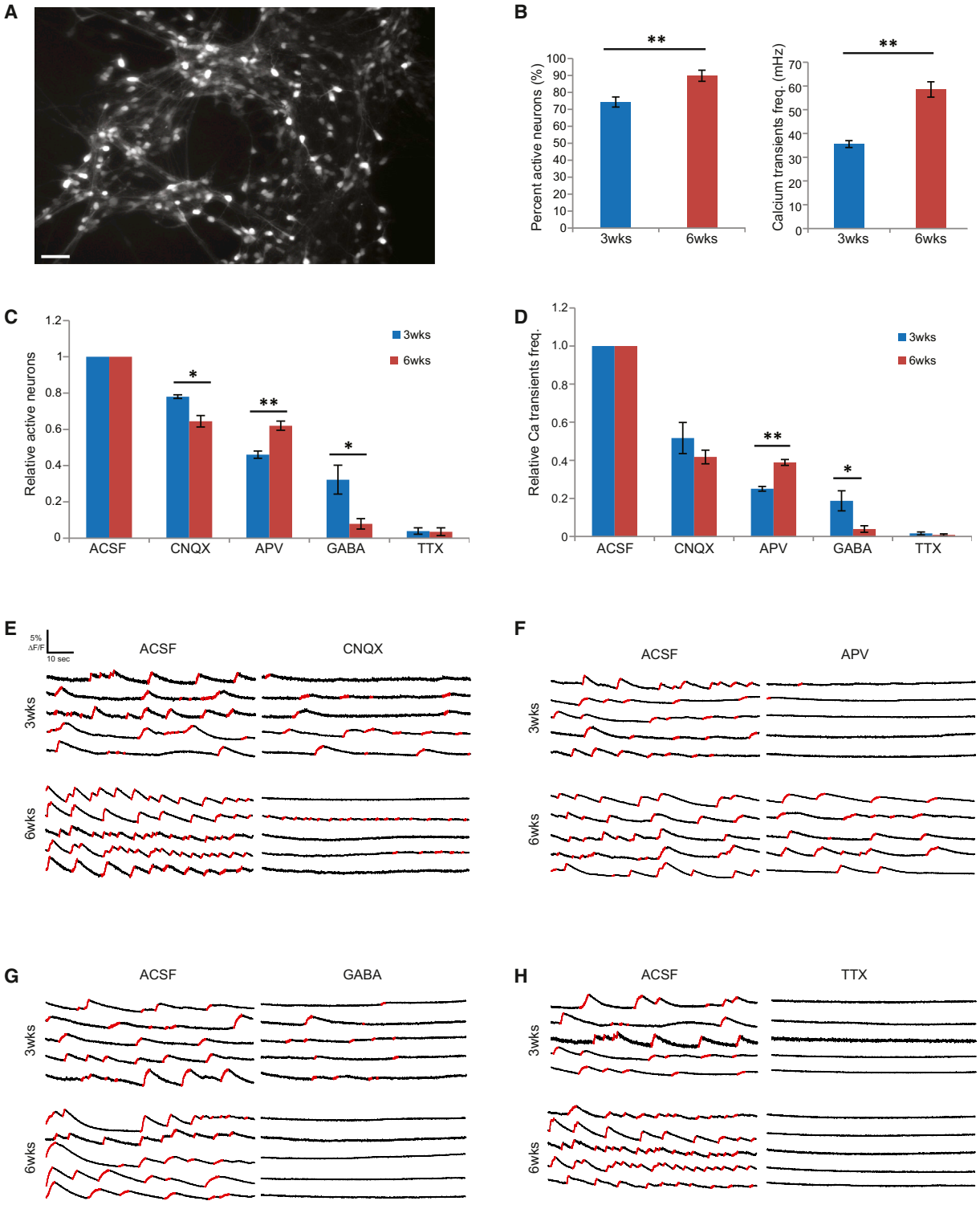

Figure 4. Calcium Imaging of hESC-Derived Hippocampal Granule Neurons at Differentiation Week 3 and Week 6

(A) Representative image of field of neurons used for calcium imaging. Scale bar, 50 μm.

(B) The percentage of active neurons and frequency of calcium transients significantly increased from week 3 to week 6, indicating formation and maturation of neuronal networks.

(legend continued on next page)

hPSCs to hippocampal granule neurons using a strategy based on developmental hallmarks. We formulated our differentiation approach to mimic the developmental cues by first using antagonists of the WNT, SHH, TGF-β, and BMP pathways to obtain a neural progenitor population patterned for the dorsal forebrain region that gives rise to the hippocampus. Then, we enriched for PROX1+ dentate granule neurons using Wnt3a, a morphogen produced by the cortical hem to establish the DG and CA subfields along the hippocampal primordial (Lee et al., 2000; Machon et al., 2007).

PROX1 expression, although highly restricted to the DG of the hippocampus in the adult brain, can also be found in additional regions of the developing brain (Torii et al., 1999; Lavado and Oliver, 2007). However, a few key findings have identified PROX1 as a suitable marker to identify the target population of DG granule neurons in our differentiation approach. First, PROX1 is uniquely found in the DG of the developing forebrain (Lavado and Oliver, 2007). Recent studies have demonstrated the feasibility of obtaining an enriched population of dorsal forebrain precursors to generate cortical pyramidal neurons from hPSCs (Shi et al., 2012a; Vanderhaeghen, 2012). Our differentiation approach extends this to identify hippocampal neural progenitors expressing FOXG1, PAX6, EMX2, and NEUROD1, which have all been shown to be critical in the development of DG (Pellegrini et al., 1996; Schwab et al., 2000; Shinozaki et al., 2004; Shen et al., 2006; Osumi et al., 2008), thus providing the rationale for using PROX1 as a reliable marker to identify our target neuronal subtype. Furthermore, the temporal expression patterns of these transcription factors during the our differentiation protocol mimic that of the hippocampal neurogenesis process observed in vivo, providing additional confidence to the identity of these PROX1+ neurons as DG granule neurons. Second, recent studies have also demonstrated the critical role for PROX1 in defining the granule neuron identity during hippocampal development. The sustained presence of PROX1 is necessary to specify the granule neuron identity relative to the CA3 pyramidal fate in the hippocampus, and the loss of Prox1 in immature DG neurons results in the manifestation of CA3 pyramidal neuronal properties (Lavado et al., 2010; Iwano et al., 2012). Our data show sustained levels of PROX1 expression from week 3 of differentiation and onward as well as double labeling of PROX1 with MAP2AB, a postmitotic neuronal marker. Finally, we also developed a new tool (lentiviral Prox1-EGFP reporter) that can be readily used to visualize and sort granule neurons in culture. Prox1-EGFP-positive neurons are electrophysiologically active, demonstrating that our protocol is indeed producing functional DG granule neurons.

In addition to recapitulating the molecular signature of hippocampal neurogenesis, we were able to capture the development of functional attributes in our neuronal population of interest. Previous work on hippocampal neurogenesis has demonstrated the importance of NMDAR-mediated activity in the integration and survival of DG granule neurons during a critical period following neuronal birth, indicating that the survival of new neurons and the resulting neural circuits are regulated in an input-dependent, cell-specific manner that enables them to play a critical role in learning and memory (Tashiro et al., 2006). Here we show that hESC-derived hippocampal granule neurons formed neuronal networks with a greater component of NMDAR-mediated neuronal activity at the early stage of differentiation, exhibiting greater inhibition of neuronal activity by APV, an antagonist of NMDARs. Conversely, these neural networks demonstrated a higher level of AMPA-receptor-mediated activity at the later stage, as indicated by incomplete inhibition of neuronal activity by CNQX, an antagonist of AMPA receptors, at the 3-week time point and complete inhibition of activities at the 6-week time point. Finally, previous studies have demonstrated that maturation of new hippocampal granule neurons progress through a GABA-excitatory stage as a result of elevated intracellular chloride concentration, denoting a transient hyperexcitatory phase in the maturation of DG granule neurons (Li et al., 2012). The neurons generated using our differentiation protocol presented spontaneous activity that was inhibited by GABA at both 3 and 6 weeks differentiation. It is conceivable that the GABA excitatory period of development precedes the time points surveyed here and that the neurons have already switched to glutamate-mediated excitatory transmission. However, a progressive increase in GABA sensitivity with maturation is consistent with existing animal studies (Ganguly et al., 2001; Li et al., 2012).

Finally, because the hippocampal DG niche can provide the necessary cues to facilitate differentiation and integration of granule neurons into the existing neural circuitry throughout adulthood, we took advantage of this system to transplant hESC-derived hippocampal NPCs into the DG and to characterize their development in the endogenous environment. Remarkably, hippocampal NPCs

(C and D) Pharmacological perturbation of the neuronal networks showed increased sensitivity to CNQX and GABA but reduced sensitivity to APV from week 3 to week 6.

(E–H) Representative traces of intracellular calcium in response to pharmacological perturbations at week 3 and week 6.

*$p < 0.05$; **$p < 0.01$. In (B)–(D), n = 15 and 16 movies (1,026 and 1,392 neurons) for 3 weeks and 6 weeks, respectively; two-tailed t test. All data are presented as mean ± SEM.

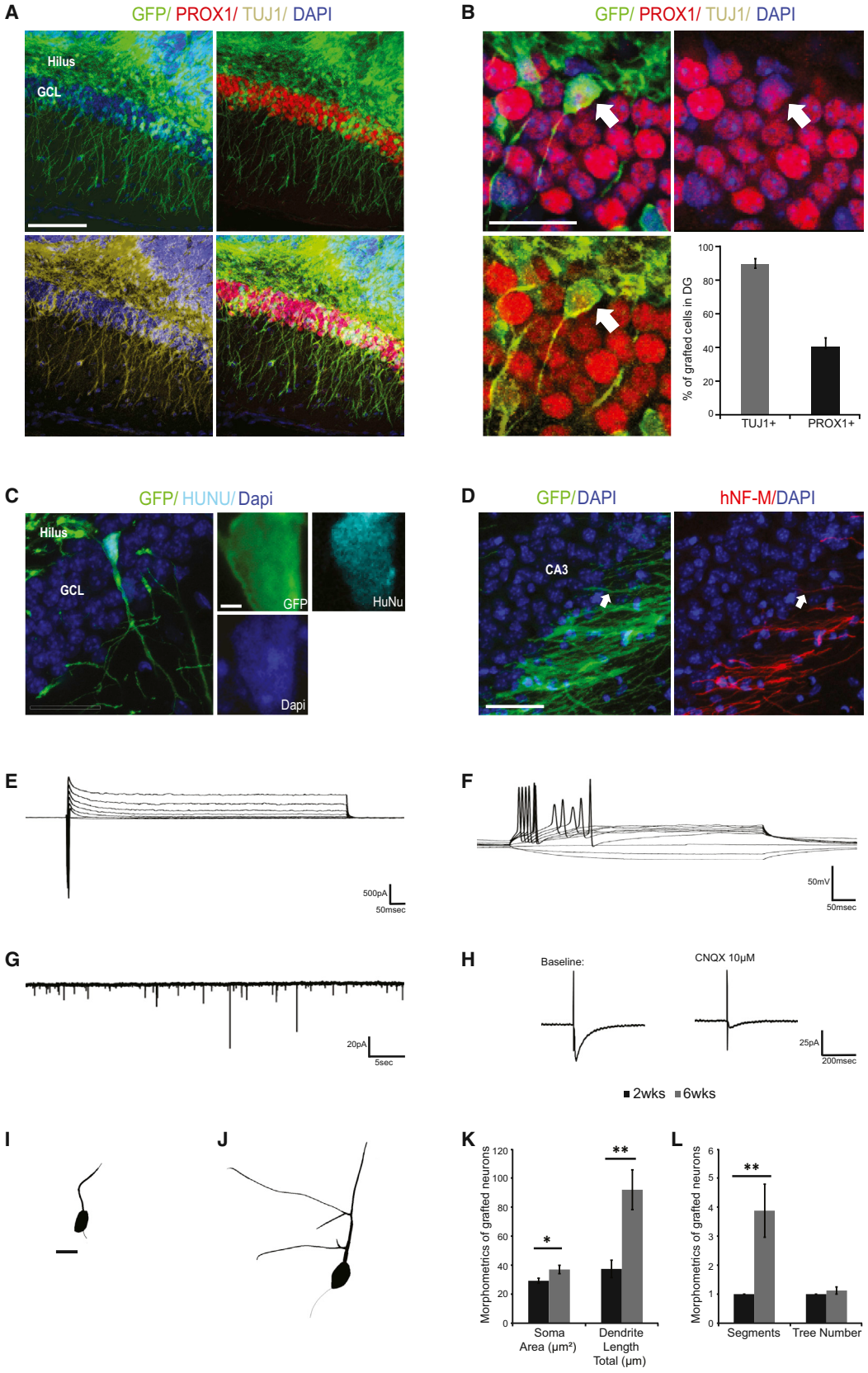

(legend on next page)

grafted to the SGZ took on the polarized morphology of immature neurons as early as 2 weeks posttransplantation and continued to develop in vivo, as evidenced by increased soma size and dendritic arborization oriented toward the entorhinal inputs at 6 weeks posttransplantation. In addition, the grafted cells exhibited spontaneous postsynaptic currents and produced EPSCs in response to stimulation of the perforant path, demonstrating integration into the hippocampal neural circuitry. In vivo grafting into the hippocampus DG could provide a more complex and comprehensive set of environmental cues for generating and assessing the development of hippocampal granule neurons and may allow for detection of more subtle morphometric differences between diseased and nondiseased neurons that would not be apparent in the in vitro setting.

As a proof-of-principle application, we investigated whether directed differentiation to hippocampal granule neurons could reveal disease-related phenotypes in the hiPSC model of SCZD, a neurodevelopmental disease in which hippocampus-associated cognitive impairments are highly conserved among the patient cohort (Tamminga et al., 2010, 2012). Studies using animal models and, more recently, postmortem brain tissue found evidence of pathophysiological alterations, termed the "immature dentate gyrus," that were characterized by an increased number of calretinin-positive immature NPCs at the expense of calbindin-positive mature neurons in SCZD and bipolar patients (Yamasaki et al., 2008; Walton et al., 2012; Shin et al., 2013). These findings provide important insights into the hypothesized neurodevelopmental etiology of these neuropsychiatric diseases. However, the approaches used thus far have significant limitations. Examining postmortem tissue can only provide information at the end point of the disease and limits investigation of developmental aspects that may have led to this pathophysiology. Moreover, transgenic animal models can only reproduce some attributes of SCZD and cannot fully recapitulate the key genetic events associated with the pathogenesis of the disease. Using our differentiation approach, we generated hippocampal granule neurons from hiPSC lines previously derived from the fibroblasts of four control and four schizophrenic individuals (Brennand et al., 2011). We first "prepatterned' the previously derived hiPSCs to DG precursors and then, using our in vitro model of hippocampal neurogenesis, found that whereas SCZD hiPSCs gave rise to a NPC population with similar levels of PAX6 and EMX2 as controls, they had reduced levels of PROX1 and NEUROD1, suggesting deficits in generating hippocampal granule neurons from the neural progenitor pool. Strikingly, functional characterization of neural networks of SCZD and control neurons using calcium imaging showed a significant reduction in the percentage of active neurons. Further investigation by electrophysiological recording of hiPSC-derived, Prox1+ neurons revealed that whereas both SCZD and control neurons displayed similar basic neuronal characteristics of Na^+/K^+ currents and evoked action potentials, SCZD neurons exhibited reduced levels of spontaneous neurotransmitter release, which may be associated with a less mature state of the neurons. Our work provides additional evidence that hippocampal neurogenesis is compromised in SCZD patients and supports the hypothesis of an immature DG in patients with SCZD. Moreover, our findings suggest that the deficit may originate in the development of the NPCs into the DG granule neurons and that the delayed maturation of SCZD DG granule neurons resulted in attenuation of functional network connectivity and activity levels in the SCZD hiPSC-derived neurons, potentially producing a non-cell-autonomous defect in the property of the hippocampal neural circuitry. Our previous study using microarray gene expression analysis indicated a deficiency in the

Figure 5. Transplantation of Hippocampal NPCs into Dentate Gyrus of P14 NOD-SCID Mice

(A) Grafted GFP+ NPCs gave rise to neurons integrated into the endogenous granule cell layer (GCL) of the DG. Scale bar, 100 μm.

(B and C) Graft-derived neurons in the GCL are positive for neuronal markers Tuj1 and Prox1 and human antigen marker HuNu. Scale bar, 50 μm; n = 3 animals.

(D) Graft-derived neurons extended processes along the endogenous mossy fiber path to CA3 region. Scale bar, 50 μm.

(E) Na^+/K^+ currents of grafted neurons in voltage clamp.

(F) Evoked action potentials in response to somatic current injection.

(G) Trace showing spontaneous postsynaptic currents in grafted neurons.

(H) Trace showing excitatory postsynaptic currents in grafted neurons in response to stimulation at perforant path. The response can be blocked by 10 μM CNQX.

(I) Representative morphology of graft-derived neurons at week 2 posttransplantation.

(J) Representative morphology of graft-derived neurons at week 6 posttransplantation. Scale bar, 10 μm.

(K) Morphometric analysis of graft-derived neurons showing increased soma size and total dendritic lengths between week 2 and week 6 posttransplantation.

(L) Morphometric analysis of graft-derived neurons showing an increased number of dendritic segments and a similar number of dendritic trees between week 2 and week 6 posttransplantation.

*$p < 0.05$; **$p < 0.01$. n = 16 neurons traced; two-tailed t test. All data are presented as mean ± SEM.

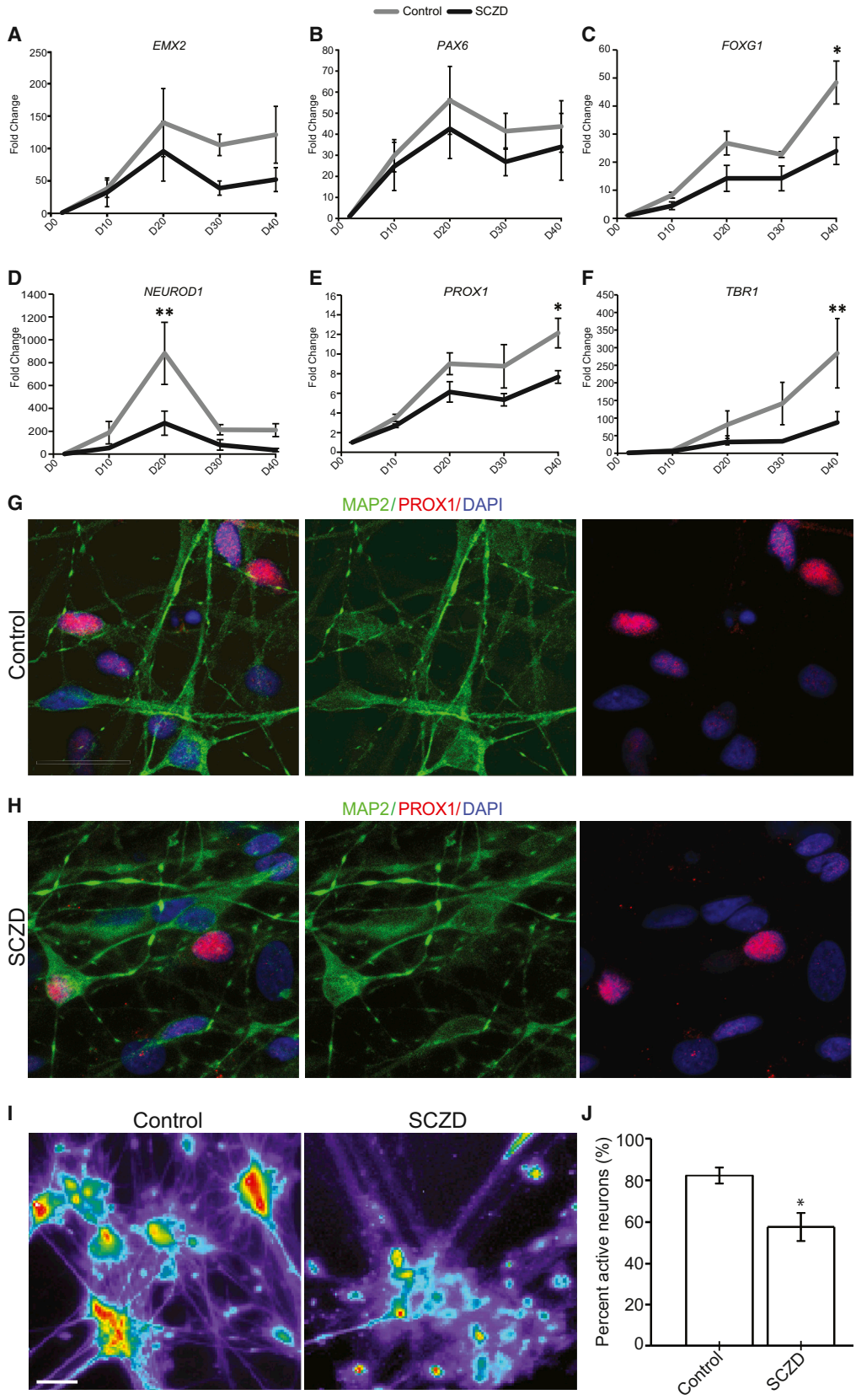

(legend on next page)

number of cellular pathways in these SCZD hiPSC-derived neurons, including in the canonical WNT/β-catenin pathway (Brennand et al. 2011). Because our differentiation approach utilizes Wnt3a to mimic conditions in the developing DG, it is conceivable that deficits observed in the SCZD neurons may be due to altered levels of WNT signaling. However, additional work is needed to verify this possibility and elucidate mechanisms that attribute to this defect. Nevertheless, the current results, together with the previous array data, support a role for WNT signaling in the generation of functional DG neurons in SCZD patients.

Here, we present the generation of DG granule neurons from hPSCs and an in vitro model that recapitulates many of the features of the process of hippocampal neurogenesis. The ability to mimic the developmental process of disease-relevant cell types in an in vitro setting is important for providing insights into the generation and the pathogenesis of CNS disorders with a strong neurodevelopmental component. Our findings are relevant to studies of human in vitro hippocampal neurogenesis and represent a promising tool for the screening of drugs that could have clinical application in a disease setting.

EXPERIMENTAL PROCEDURES

Cell Culture

SCZD and control hiPSCs were derived and characterized as previously described (Brennand et al., 2011). hiPSC colonies were kept in feeder-free conditions and passed using mechanical dissociation. EBs were formed by mechanical dissociation of hiPSC colonies using collagenase and plating onto low-adherence dishes in hESC medium without fibroblast growth factor 2 (FGF2). For EB differentiation, floating EBs were treated with DKK1 (0.5 μg/ml), SB431542 (10 μM), Noggin (0.5 μg/ml), and cyclopamine (1 μM) in Dulbecco's modified Eagle's medium (DMEM)/F12 (Invitrogen) plus N2 and B27 for 20 days followed by Wnt3a (20 ng/ml) and BDNF (20 ng/ml) in DMEM/F12 plus N2 and B27 for 20 days. The EBs were dissociated with Papain and DNase (Worthington) for 1 hr at 37°C and plated onto a monolayer of human hippocampal astrocytes (ScienCell). To obtain NPCs, EBs treated with DKK1/SB431542/Noggin/cyclopamine were plated after 20 days onto polyornithine/laminin (Sigma)-coated dishes in DMEM/F12 (Invitrogen) plus N2. Rosettes were manually collected and dissociated with Accutase (Chemicon) after 1 week and plated onto coated dishes with NPC media (DMEM/F12, N2, B27, and FGF2). To obtain mature neurons, NPCs were plated on a monolayer of hippocampal astrocytes in the presence of DMEM/F12, N2, B27, ascorbic acid (200 nM), cyclic AMP (cAMP; 500 μg/ml), laminin (1 μg/ml), BDNF (20 ng/ml), Wnt3a (20 ng/ml), and 1% fetal bovine serum for 3 weeks. Wnt3a was removed after 3 weeks.

Immunocytochemistry

Cells were fixed in 4% paraformaldehyde and then permeabilized with 0.25% Triton X-100 in PBS. Cells were blocked in PBS containing 0.25% Triton X-100 and 10% donkey serum. Antibodies and quantification methods used are described in the Supplemental Experimental Procedures. Fluorescent signals were detected using a Zeiss 710 laser scanning microscope and images were processed with ZEN 2011.

RNA Extraction and qRT-PCR

Total cellular RNA was extracted from ~5 × 10^6 cells using the RNA-BEE (QIAGEN), according to the manufacturer's instructions, and reverse transcribed using the high-capacity cDNA synthesis kit from AB Biosystems. qPCR was done using SYBR green (Life Technologies). qPCR results were analyzed using SDS Software v 3.2 for 7900HT real-time PCR system. Primer sequences used are described in the Supplemental Experimental Procedures.

Calcium Imaging

Neuronal networks derived from hESCs and hiPSCs were infected with the Synapsin-DsRed lentiviral vector. Cell cultures were incubated with 2–5 μM Fluo-4AM (Molecular Probes/Invitrogen) for 40 min at room temperature. The threshold for activity was set at the 95th percentile of the amplitude for all detected events. Images were acquired with MetaMorph 7.7 (MDS Analytical Technologies) and processed using ImageJ (http://rsbweb.nih.gov/ij/) and custom-written routines in Matlab 7.2 (Mathworks).

Figure 6. Reduced Levels of Hippocampal Neurogenesis from SCZD NPCs

(A–C) qPCR for genes expressed in hippocampal NPCs revealed comparable levels of *EMX2* and *PAX6* but reduced levels of *FOXG1* in SCZD hiPSC lines differentiated using the EB method.

(D–F) PCR for genes expressed in hippocampal granule neurons showed reduced levels of *NEUROD1*, *PROX1*, and *TBR1* in SCZD hiPSC lines differentiated using the EB method.

(G and H) Representative images of immunostaining for Prox1+ neurons dissociated from EBs at differentiation day 40 and cocultured with hippocampal astrocytes for 4 weeks. Scale bar, 50 μm.

(I) Pseudocolored images showing increases in florescent intensities of Fluo-4AM calcium indicator in control and SCZD neural networks. Scale bar, 50 μm.

(J) The number of neurons with calcium transients is normalized to the total neurons imaged in each field of view as indicated with lentiviral synapsin/red fluorescent protein. The percentage of active neurons significantly decreased in SCZD neural networks.

*$p < 0.05$; **$p < 0.01$. In (A)–(F), n = 4 SCZD lines and 4 control lines with three biological replicates done for each line, two-way ANOVA and Bonferroni post hoc test. In (J), *$p < 0.05$, n = 4 SCZD lines and 4 control lines, n = 20 and 22 wells imaged for SCZD and control lines (four to seven wells per line), respectively; two-tailed t test. Data are presented as mean ± SEM.

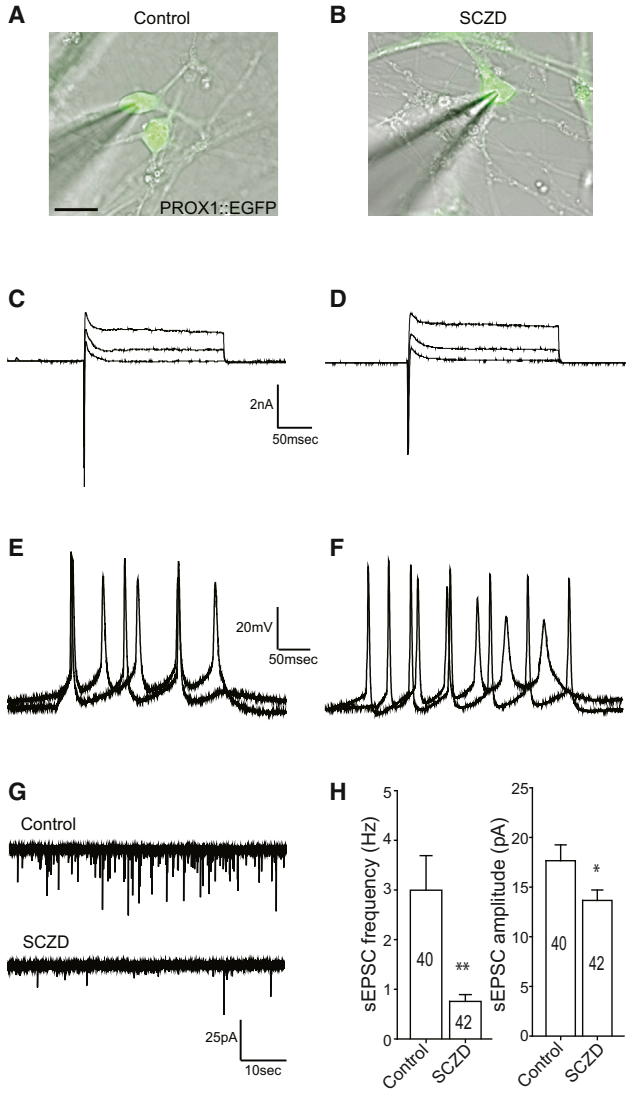

Figure 7. Attenuated Spontaneous Neurotransmitter Release in SCZD Neurons

(A and B) Fluorescence micrographs of representative control (A) and SCZD (B) neurons labeled with the *PROX1-EGFP* lentiviral vector. Scale bar, 15 μm.

(C–F) Electrophysiological properties of control and SCZD neurons; transient Na^+ currents and sustained K^+ currents in response to voltage step depolarizations in control (C) and SCZD (D) neurons (command voltage varied from −20 to +30 mV in 5 mV increments when cells were voltage-clamped at −70 mV); action potentials evoked by somatic current injections in control (E) and SCZD (F) neurons (cells current-clamped at −60 mV, injected currents from 10 to 20 pA).

(G) Representative traces of spontaneous postsynaptic currents in control and SCZD neurons.

(H) Quantification of the frequency and amplitude of postsynaptic currents in control and SCZD neurons. *$p < 0.05$, **$p < 0.01$; $n = 40$ control neurons, 42 SCZD neurons; two-tailed t test. Data are presented as mean ± SEM.

Electrophysiology

Whole-cell patch-clamp recordings were performed from cells cocultured with astrocytes after 6 weeks of differentiation. The bath was constantly perfused with artificial cerebrospinal fluid (ACSF) (115 mM NaCl, 2 mM KCl, 3 mM CaCl2, 10 mM glucose, and 1.5 mM MgCl2). The recording micropipettes (tip resistance 3–6 MΩ) were filled with internal solution (140 mM K-gluconate, 5 mM KCl, 2 mM $MgCl_2$, 0.2 mM EGTA, 2.5 mM Na-ATP, 0.5 mM Na-GTP, and 10 mM Na_2-phosphocreatine). Additional details are provided in the Supplemental Experimental Procedures. Statistical comparisons of wild-type and SZCD groups were made using the nonparametric Kolmogorov-Smirnov two-tailed test, with a significance criterion of $p = 0.05$.

In Vivo Transplantation

All experimental procedures were approved by the Institutional Animal Care and Use Committee at The Salk Institute for Biological Studies. For the engrafting assay, NPCs infected with lentiviral vector carrying the CAG-GFP reporter construct were dissociated and resuspended in PBS-glucose + ROCK inhibitor, BDNF, ascorbic acid, cAMP, and laminin at 20,000 cells per μl. P14 NOD-SCID pups were anesthetized using ketamine/xylazine (100 mg/kg, 10 mg/kg) and 1 μl of cell suspension was delivered to the DG of the mouse hippocampus in the right hemisphere by stereotaxic surgery. The injection site was determined using the difference between bregma and lambda (d), using the position of the bregma as reference as follows: anteroposterior, $-(1/2) \times d$ mm; lateral, −1.6 mm (if $d < 1.6$) or −1.7 mm; ventral, −1.9 mm (from dura). Then 2 or 4 weeks posttransplantation, animals were anesthetized with ketamine/xylazine and perfused transcardially with 0.9% saline followed by 4% paraformaldehyde. The brain samples were postfixed with 4% paraformaldehyde and equilibrated in 30% sucrose. Coronal sections of 40 μm were prepared with a sliding microtome. Brain sections of one-in-four series were selected for immunostaining. Neurons in the granular layer of the DG were traced on an upright stereoinvestigator microscope (maker) under 40× objective and morphometric analyses were done using Neurolucida (MBF Bioscience).

SUPPLEMENTAL INFORMATION

Supplemental Information includes Supplemental Experimental Procedures, two figures, and one table and can be found with this article online at http://dx.doi.org/10.1016/j.stemcr.2014.01.009.

ACKNOWLEDGMENTS

This work was supported by the CIRM (grant RL1-00649), the Annette C. Merle-Smith and Mathers Foundation, The Leona M. and Harry B. Helmsley Charitable Trust, Sanofi-Aventis, and generous donations from Mary Jane & Robert Engman.

Received: December 27, 2013
Revised: January 17, 2014
Accepted: January 20, 2014
Published: February 27, 2014

REFERENCES

Brennand, K.J., Simone, A., Jou, J., Gelboin-Burkhart, C., Tran, N., Sangar, S., Li, Y., Mu, Y., Chen, G., Yu, D., et al. (2011). Modelling schizophrenia using human induced pluripotent stem cells. Nature *473*, 221–225.

Di Giorgio, F.P., Boulting, G.L., Bobrowicz, S., and Eggan, K.C. (2008). Human embryonic stem cell-derived motor neurons are sensitive to the toxic effect of glial cells carrying an ALS-causing mutation. Cell Stem Cell *3*, 637–648.

Dimos, J.T., Rodolfa, K.T., Niakan, K.K., Weisenthal, L.M., Mitsumoto, H., Chung, W., Croft, G.F., Saphier, G., Leibel, R., Goland, R., et al. (2008). Induced pluripotent stem cells generated from patients with ALS can be differentiated into motor neurons. Science *321*, 1218–1221.

Erickson, K.I., Prakash, R.S., Voss, M.W., Chaddock, L., Heo, S., McLaren, M., Pence, B.D., Martin, S.A., Vieira, V.J., Woods, J.A., et al. (2010). Brain-derived neurotrophic factor is associated with age-related decline in hippocampal volume. J. Neurosci. *30*, 5368–5375.

Ganguly, K., Schinder, A.F., Wong, S.T., and Poo, M. (2001). GABA itself promotes the developmental switch of neuronal GABAergic responses from excitation to inhibition. Cell *105*, 521–532.

Gao, Z., Ure, K., Ables, J.L., Lagace, D.C., Nave, K.A., Goebbels, S., Eisch, A.J., and Hsieh, J. (2009). Neurod1 is essential for the survival and maturation of adult-born neurons. Nat. Neurosci. *12*, 1090–1092.

Gaspard, N., Bouschet, T., Hourez, R., Dimidschstein, J., Naeije, G., van den Ameele, J., Espuny-Camacho, I., Herpoel, A., Passante, L., Schiffmann, S.N., et al. (2008). An intrinsic mechanism of corticogenesis from embryonic stem cells. Nature *455*, 351–357.

Hagihara, H., Takao, K., Walton, N.M., Matsumoto, M., and Miyakawa, T. (2013). Immature dentate gyrus: an endophenotype of neuropsychiatric disorders. Neural Plast. *2013*, 318596.

Hodge, R.D., Kahoud, R.J., and Hevner, R.F. (2012). Transcriptional control of glutamatergic differentiation during adult neurogenesis. Cell. Mol. Life Sci. *69*, 2125–2134.

Hollrigel, G.S., and Soltesz, I. (1997). Slow kinetics of miniature IPSCs during early postnatal development in granule cells of the dentate gyrus. J. Neurosci. *17*, 5119–5128.

Hsieh, J. (2012). Orchestrating transcriptional control of adult neurogenesis. Genes Dev. *26*, 1010–1021.

Hu, B.Y., Weick, J.P., Yu, J., Ma, L.X., Zhang, X.Q., Thomson, J.A., and Zhang, S.C. (2010). Neural differentiation of human induced pluripotent stem cells follows developmental principles but with variable potency. Proc. Natl. Acad. Sci. USA *107*, 4335–4340.

Iwano, T., Masuda, A., Kiyonari, H., Enomoto, H., and Matsuzaki, F. (2012). Prox1 postmitotically defines dentate gyrus cells by specifying granule cell identity over CA3 pyramidal cell fate in the hippocampus. Development *139*, 3051–3062.

Jessberger, S., Zhao, C., Toni, N., Clemenson, G.D., Jr., Li, Y., and Gage, F.H. (2007). Seizure-associated, aberrant neurogenesis in adult rats characterized with retrovirus-mediated cell labeling. J. Neurosci. *27*, 9400–9407.

Karalay, O., Doberauer, K., Vadodaria, K.C., Knobloch, M., Berti, L., Miquelajauregui, A., Schwark, M., Jagasia, R., Taketo, M.M., Tarabykin, V., et al. (2011). Prospero-related homeobox 1 gene (Prox1) is regulated by canonical Wnt signaling and has a stage-specific role in adult hippocampal neurogenesis. Proc. Natl. Acad. Sci. USA *108*, 5807–5812.

Kopper, O., Giladi, O., Golan-Lev, T., and Benvenisty, N. (2010). Characterization of gastrulation-stage progenitor cells and their inhibitory crosstalk in human embryoid bodies. Stem Cells *28*, 75–83.

Kriks, S., Shim, J.W., Piao, J., Ganat, Y.M., Wakeman, D.R., Xie, Z., Carrillo-Reid, L., Auyeung, G., Antonacci, C., Buch, A., et al. (2011). Dopamine neurons derived from human ES cells efficiently engraft in animal models of Parkinson's disease. Nature *480*, 547–551.

Kuwabara, T., Hsieh, J., Muotri, A., Yeo, G., Warashina, M., Lie, D.C., Moore, L., Nakashima, K., Asashima, M., and Gage, F.H. (2009). Wnt-mediated activation of NeuroD1 and retro-elements during adult neurogenesis. Nat. Neurosci. *12*, 1097–1105.

Lavado, A., and Oliver, G. (2007). Prox1 expression patterns in the developing and adult murine brain. Dev. Dyn. *236*, 518–524.

Lavado, A., Lagutin, O.V., Chow, L.M., Baker, S.J., and Oliver, G. (2010). Prox1 is required for granule cell maturation and intermediate progenitor maintenance during brain neurogenesis. PLoS Biol. *8*, e1000460.

Lee, S.M., Tole, S., Grove, E., and McMahon, A.P. (2000). A local Wnt-3a signal is required for development of the mammalian hippocampus. Development *127*, 457–467.

Li, Y., Aimone, J.B., Xu, X., Callaway, E.M., and Gage, F.H. (2012). Development of GABAergic inputs controls the contribution of maturing neurons to the adult hippocampal network. Proc. Natl. Acad. Sci. USA *109*, 4290–4295.

Liu, M., Pleasure, S.J., Collins, A.E., Noebels, J.L., Naya, F.J., Tsai, M.J., and Lowenstein, D.H. (2000). Loss of BETA2/NeuroD leads to malformation of the dentate gyrus and epilepsy. Proc. Natl. Acad. Sci. USA *97*, 865–870.

Ma, L., Liu, Y., and Zhang, S.C. (2011). Directed differentiation of dopamine neurons from human pluripotent stem cells. Methods Mol. Biol. *767*, 411–418.

Machon, O., Backman, M., Machonova, O., Kozmik, Z., Vacik, T., Andersen, L., and Krauss, S. (2007). A dynamic gradient of Wnt signaling controls initiation of neurogenesis in the mammalian cortex and cellular specification in the hippocampus. Dev. Biol. *311*, 223–237.

Marchetto, M.C., Muotri, A.R., Mu, Y., Smith, A.M., Cezar, G.G., and Gage, F.H. (2008). Non-cell-autonomous effect of human SOD1 G37R astrocytes on motor neurons derived from human embryonic stem cells. Cell Stem Cell *3*, 649–657.

Maroof, A.M., Keros, S., Tyson, J.A., Ying, S.W., Ganat, Y.M., Merkle, F.T., Liu, B., Goulburn, A., Stanley, E.G., Elefanty, A.G., et al. (2013). Directed differentiation and functional maturation of cortical interneurons from human embryonic stem cells. Cell Stem Cell *12*, 559–572.

Mateus-Pinheiro, A., Pinto, L., Bessa, J.M., Morais, M., Alves, N.D., Monteiro, S., Patrício, P., Almeida, O.F., and Sousa, N. (2013).

Sustained remission from depressive-like behavior depends on hippocampal neurogenesis. Transcult. Psychiatry *3*, e210.

Miyata, T., Maeda, T., and Lee, J.E. (1999). NeuroD is required for differentiation of the granule cells in the cerebellum and hippocampus. Genes Dev. *13*, 1647–1652.

Nicholas, C.R., Chen, J., Tang, Y., Southwell, D.G., Chalmers, N., Vogt, D., Arnold, C.M., Chen, Y.J., Stanley, E.G., Elefanty, A.G., et al. (2013). Functional maturation of hPSC-derived forebrain interneurons requires an extended timeline and mimics human neural development. Cell Stem Cell *12*, 573–586.

Osumi, N., Shinohara, H., Numayama-Tsuruta, K., and Maekawa, M. (2008). Concise review: Pax6 transcription factor contributes to both embryonic and adult neurogenesis as a multifunctional regulator. Stem Cells *26*, 1663–1672.

Pellegrini, M., Mansouri, A., Simeone, A., Boncinelli, E., and Gruss, P. (1996). Dentate gyrus formation requires Emx2. Development *122*, 3893–3898.

Perrier, A.L., Tabar, V., Barberi, T., Rubio, M.E., Bruses, J., Topf, N., Harrison, N.L., and Studer, L. (2004). Derivation of midbrain dopamine neurons from human embryonic stem cells. Proc. Natl. Acad. Sci. USA *101*, 12543–12548.

Reif, A., Fritzen, S., Finger, M., Strobel, A., Lauer, M., Schmitt, A., and Lesch, K.P. (2006). Neural stem cell proliferation is decreased in schizophrenia, but not in depression. Mol. Psychiatry *11*, 514–522.

Roy, N.S., Cleren, C., Singh, S.K., Yang, L., Beal, M.F., and Goldman, S.A. (2006). Functional engraftment of human ES cell-derived dopaminergic neurons enriched by coculture with telomerase-immortalized midbrain astrocytes. Nat. Med. *12*, 1259–1268.

Sahay, A., and Hen, R. (2007). Adult hippocampal neurogenesis in depression. Nat. Neurosci. *10*, 1110–1115.

Scharfman, H., Goodman, J., Macleod, A., Phani, S., Antonelli, C., and Croll, S. (2005). Increased neurogenesis and the ectopic granule cells after intrahippocampal BDNF infusion in adult rats. Exp. Neurol. *192*, 348–356.

Schwab, M.H., Bartholomae, A., Heimrich, B., Feldmeyer, D., Druffel-Augustin, S., Goebbels, S., Naya, F.J., Zhao, S., Frotscher, M., Tsai, M.J., and Nave, K.A. (2000). Neuronal basic helix-loop-helix proteins (NEX and BETA2/Neuro D) regulate terminal granule cell differentiation in the hippocampus. J. Neurosci. *20*, 3714–3724.

Shen, L., Nam, H.S., Song, P., Moore, H., and Anderson, S.A. (2006). FoxG1 haploinsufficiency results in impaired neurogenesis in the postnatal hippocampus and contextual memory deficits. Hippocampus *16*, 875–890.

Shi, Y., Kirwan, P., and Livesey, F.J. (2012a). Directed differentiation of human pluripotent stem cells to cerebral cortex neurons and neural networks. Nat. Protoc. *7*, 1836–1846.

Shi, Y., Kirwan, P., Smith, J., Robinson, H.P., and Livesey, F.J. (2012b). Human cerebral cortex development from pluripotent stem cells to functional excitatory synapses. Nat. Neurosci. *15*, 477–486.

Shin, R., Kobayashi, K., Hagihara, H., Kogan, J.H., Miyake, S., Tajinda, K., Walton, N.M., Gross, A.K., Heusner, C.L., Chen, Q., et al. (2013). The immature dentate gyrus represents a shared phenotype of mouse models of epilepsy and psychiatric disease. Bipolar Disord. Published online April 6, 2013. http://dx.doi.org/10.1111/bdi.12064.

Shinozaki, K., Yoshida, M., Nakamura, M., Aizawa, S., and Suda, Y. (2004). Emx1 and Emx2 cooperate in initial phase of archipallium development. Mech. Dev. *121*, 475–489.

Spitzer, N.C., Root, C.M., and Borodinsky, L.N. (2004). Orchestrating neuronal differentiation: patterns of Ca2+ spikes specify transmitter choice. Trends Neurosci. *27*, 415–421.

Steinbeck, J.A., Koch, P., Derouiche, A., and Brüstle, O. (2012). Human embryonic stem cell-derived neurons establish region-specific, long-range projections in the adult brain. Cell. Mol. Life Sci. *69*, 461–470.

Tamminga, C.A., Stan, A.D., and Wagner, A.D. (2010). The hippocampal formation in schizophrenia. Am. J. Psychiatry *167*, 1178–1193.

Tamminga, C.A., Thomas, B.P., Chin, R., Mihalakos, P., Youens, K., Wagner, A.D., and Preston, A.R. (2012). Hippocampal novelty activations in schizophrenia: disease and medication effects. Schizophr. Res. *138*, 157–163.

Tashiro, A., Sandler, V.M., Toni, N., Zhao, C., and Gage, F.H. (2006). NMDA-receptor-mediated, cell-specific integration of new neurons in adult dentate gyrus. Nature *442*, 929–933.

Tatebayashi, Y., Lee, M.H., Li, L., Iqbal, K., and Grundke-Iqbal, I. (2003). The dentate gyrus neurogenesis: a therapeutic target for Alzheimer's disease. Acta Neuropathol. *105*, 225–232.

Torii, Ma., Matsuzaki, F., Osumi, N., Kaibuchi, K., Nakamura, S., Casarosa, S., Guillemot, F., and Nakafuku, M. (1999). Transcription factors Mash-1 and Prox-1 delineate early steps in differentiation of neural stem cells in the developing central nervous system. Development *126*, 443–456.

Vanderhaeghen, P. (2012). Generation of cortical neurons from pluripotent stem cells. Prog. Brain Res. *201*, 183–195.

Walton, N.M., Zhou, Y., Kogan, J.H., Shin, R., Webster, M., Gross, A.K., Heusner, C.L., Chen, Q., Miyake, S., Tajinda, K., et al. (2012). Detection of an immature dentate gyrus feature in human schizophrenia/bipolar patients. Transcult. Psychiatry *2*, e135.

Watanabe, K., Kamiya, D., Nishiyama, A., Katayama, T., Nozaki, S., Kawasaki, H., Watanabe, Y., Mizuseki, K., and Sasai, Y. (2005). Directed differentiation of telencephalic precursors from embryonic stem cells. Nat. Neurosci. *8*, 288–296.

Wexler, E.M., Paucer, A., Kornblum, H.I., Palmer, T.D., and Geschwind, D.H. (2009). Endogenous Wnt signaling maintains neural progenitor cell potency. Stem Cells *27*, 1130–1141.

Yamasaki, N., Maekawa, M., Kobayashi, K., Kajii, Y., Maeda, J., Soma, M., Takao, K., Tanda, K., Ohira, K., Toyama, K., et al. (2008). Alpha-CaMKII deficiency causes immature dentate gyrus, a novel candidate endophenotype of psychiatric disorders. Mol. Brain *1*, 6.

Zhao, C., Deng, W., and Gage, F.H. (2008). Mechanisms and functional implications of adult neurogenesis. Cell *132*, 645–660.